scientific reports

Check for updates

OPEN

"5,7,4'-trimethoxyflavanone from *Bauhinia variegata* exerts anti-inflammatory and protective actions in LPS-challenged rat intestine"

Peramaiyan Rajendran[1]✉, Balasubramanian Rajkapoor[2], Maryam N. AlNasser[1], Gamal M. Bekhet[1], Ramya Sekar[3]✉, Lalitha Keddal Govindaram[4] & Faten Abdullah Alrashaid[5]

This study aimed to investigate the protective effects of 5,7,4'-trimethoxyflavanone (TMF), a bioactive compound isolated from *Bauhinia variegata* Linn., on lipopolysaccharide (LPS)-induced intestinal injury in rats. Chronic intestinal inflammation was induced by repeated LPS administration, and the therapeutic potential of TMF in alleviating the associated damage was assessed. Male rats were subjected to chronic intestinal inflammation via repeated intraperitoneal administration of LPS at a dose of 1 mg/kg body weight once daily for 4 weeks. Simultaneously, the test group received daily oral administration of TMF at 75 mg/kg body weight from day one after 4 weeks of induction of intestinal inflammation until the end of the experiment. Histopathological examination of the intestines, along with biochemical assays for inflammatory markers, oxidative stress, and tissue integrity, were performed to evaluate the protective effects of TMF. Comparisons between the LPS-treated control group and the TMF-treated group were made to assess the reductions in inflammation and intestinal injury. TMF therapy diminished LPS-induced Nuclear Factor kappa B(NF-κB) activation and inhibited the levels of TNF-α, IL-6, and IL-1β, thereby reducing oxidative stress. These data indicate that TMF provides protective effects by regulating critical inflammatory and oxidative processes associated with LPS-induced intestinal damage. In conclusion, TMF from *B. variegata* has been demonstrated to be a potential therapeutic agent for mitigating intestinal inflammation and oxidative damage, suggesting a natural method for addressing inflammation-induced gut lesions. Additional research is necessary to investigate its clinical applicability in inflammatory bowel disease and other gastrointestinal conditions.

Keywords Inflammation, Intestine, LPS, Oxidative stress, 5,7,4'-trimethoxyflavanone

Intestinal inflammation and injury are significant clinical concerns associated with various disorders, including inflammatory bowel disease (IBD), sepsis-associated enteropathy, and systemic inflammatory response syndrome (SIRS). These conditions contribute substantially to morbidity worldwide due to their chronic nature and the critical role of the intestine in nutrient absorption and immune regulation. The pathogenesis often involves the overactivation of immune pathways triggered by bacterial endotoxins such as lipopolysaccharide (LPS), a major component of the outer membrane of gram-negative bacteria[1,2]. LPS activates nuclear factor kappa B (NF-κB)

[1]Department of Biological Sciences, College of Science, King Faisal University, 31982 Al-Ahsa, Saudi Arabia. [2]Faculty of Pharmacy, Karpagam Academy of Higher Education, Eachanari Post, Coimbatore 641 021, India. [3]Department of Oral & Maxillofacial Pathology and Oral Microbiology, Meenakshi Ammal Dental College & Hospital, Meenakshi Academy of Higher Education and Research (Deemed to Be University), Alapakkam Main Road, Maduravoyal, Chennai, Tamil Nadu 600095, India. [4]Department of Pharmaceutical Chemistry, Ultra College of Pharmacy, , The Tamil Nadu Dr MGR Medical University, Thasildhar Nagar, Madurai,Chennai, India. [5]Deptartment of Anatomy, College of Veterinary Medicine, King Faisal University, 31982 Al-Ahsa, Saudi Arabia. ✉email: prajendran@kfu.edu.sa; drramya.oralpathology@madch.edu.in

signaling, leading to the release of proinflammatory cytokines, including tumor necrosis factor-alpha (TNF-α), interleukin-6 (IL-6), and interleukin-1 beta (IL-1β). This immune response not only contributes to inflammation but also induces oxidative stress, damaging lipids, proteins, and DNA while disrupting tight junctions between epithelial cells[3,4]. The resultant increase in intestinal permeability facilitates leaky gut syndrome, exacerbating tissue injury and dysfunction.

Despite advances in anti-inflammatory and antioxidant therapies, effective management of intestinal inflammation remains a challenge due to issues like limited efficacy, adverse effects, and poor bioavailability of many pharmacological agents[5]. In this context, natural compounds, particularly flavonoids, have gained attention for their dual antioxidant and anti-inflammatory properties. Flavonoids such as quercetin, kaempferol, and luteolin have been extensively explored for their ability to modulate the NF-κB pathway and suppress cytokine production, demonstrating protective effects in oxidative stress-induced tissue injury models. However, their clinical utility is often hindered by low stability, bioavailability, and targeted efficacy[6].

5,7,4'-Trimethoxyflavanone (TMF), a methoxylated flavonoid isolated from Bauhinia variegata Linn., presents as a promising candidate to overcome these limitations[7–9]. The additional methoxy groups in TMF's structure enhance its lipophilicity, potentially improving cellular uptake and bioavailability compared to hydroxylated flavonoids. Methoxylated flavonoids have also been reported to exhibit superior pharmacokinetics and enhanced anti-inflammatory properties[10–12]. Bauhinia variegata, widely employed in traditional medicine, is known for its anti-inflammatory, antioxidant, and hepatoprotective effects[13,14]. Nonetheless, the protective role of TMF specifically in LPS-induced intestinal oxidative stress and inflammation has not been adequately investigated, representing a critical gap in knowledge[15].

This study employs the well-established LPS-induced rat model of intestinal inflammation to evaluate the efficacy of TMF in mitigating oxidative stress and intestinal damage[16]. We chose this model to reflect the pathophysiological mechanisms underpinning endotoxin-induced intestinal injury in clinical conditions such as sepsis and IBD. By assessing key inflammatory and oxidative markers, including IL-6, IL-1β, TNF-α, NF-κB, and reactive oxygen species (ROS), this study aims to elucidate the mechanistic pathways through which TMF exerts its protective effects[17]. Understanding these mechanisms may provide valuable insights into the development of TMF as a novel therapeutic agent for treating inflammation-driven intestinal disorders.

Overall, this investigation seeks to bridge the gap between traditional medicinal knowledge and modern pharmacological research by exploring TMF's potential as a natural, effective, and bioavailable flavonoid for preventing LPS-induced intestinal inflammation and oxidative damage. Findings from this study could contribute to the advancement of phytochemical-based strategies for managing gastrointestinal inflammatory diseases, highlighting TMF as a promising scaffold for future drug development.

Materials and methods

Chemicals

LPS was acquired from Sigma–Aldrich Co. (USA). PBS, PVDF, tissue lysis buffer, a BCA protein assay kit, PAGE running buffer (10×), TBST, and a Chemiluminescence (ECL) Plus kit were acquired from Beyotime Institute of Biotechnology (Shanghai, China). This study utilized LPS from Escherichia coli O111:B4, sourced from Sigma–Aldrich (Cat. No. L2630), to induce intestinal inflammation.

Collection and authentication of plant material

The stems of Bauhinia variegata were collected from areas around the Erode district, Tamil Nadu, India, in February 2024. The plant material was taxonomically identified by the Botanical Survey of India, Coimbatore, Tamil Nadu, India. A voucher specimen (CBV-06) is kept in our laboratory for future reference.

Preparation of TMF

Extraction and isolation

The alcohol extract of *Bauhinia variegata* was fractionated using benzene (3 × 300 ml), diethyl ether (3 × 300 ml), and ethyl acetate (4 × 300 ml). The ethyl acetate fraction yielded a yellow solid, which was nonhomogeneous according to TLC and hence was subjected to separation and purification via column chromatography[18].

Column chromatographic analysis

The ethyl acetate fraction (15 g) of *Bauhinia variegata* was chromatographed on a silica gel column (60–120 mesh, 300 g, 100 × 5 cm) via gradient elution with solvents of increasing polarity. Fractions of 100 ml were collected each time, and the homogeneity of the residue was examined via TLC with suitable solvents. The details of these fractions and their characteristics are given in Table 1.

Upon concentration, fractions 1–5, 6–11, 12–19, 20–30, 31–42, 43–52, 53–60, and 61–70 presented yellowish solids. As they were mixtures and because the amounts were too small, further purification was not carried out. Upon concentration, fractions 71–81 yielded a pure yellowish solid, which was designated the compound. This yellow solid was pink according to Shinoda's test. The Rf values of the compounds in various solvent systems are given in Table 2. The compounds were subjected to spectral analysis, such as NMR and mass spectrometry, to identify the compounds[19].

The compound yielded m.f. $C_{18}H_{18}O_5$, m.p. 205 °C, (M) + 314 (EIMS). UV (MeOH): 283, 320; (+ NaOMe): 283, 330; (+ NaOAc): 283, 315; 372; (+ NaOAc–H3BO3): 283, 315, 372; (+ AlCl3): 283, 315; (+ AlCl3–HCl): 282, 315. 1H-NMR (400 MHz–CDCl3), δ 7.18 (2H, d, J = 8.5 Hz, 2`, 6` of ring B), 6.61 (2H, d, J = 8.5 Hz, 3`,5` of ring B), 6.12 (1H, d, J = 2.5 Hz, H-8 of ring A), 5.95 (1H, d, J = 2.5 Hz, H-6 of ring A), 5.26 (1H, dd, J = 13.0, 3.0 Hz. H-2 of ring C), 4.09 (3H, s, OCH3 group), 3.9 (3H, s, OCH3), 3.74 (3H, s, OCH3), 2.89 (1H, dd, J = 17.0, 3.0 Hz, H-3 of ring C), 2.81 (1H, dd, J = 17.0, 3.0 Hz, H-3 of ring C). 13C-NMR (100 MHz–CDCl3), 79.8 (C–2), 45.3 (C–

Fraction collected	% Eluent composition	Remarks
1–5	100 hexane	Waxy substance
6–11	90/10 hexane/EtOAc	Waxy substance
12–19	80/20 hexane/EtOAc	Yellowish green solid
20–30	70/30 hexane/EtOAc	Pale yellow solid
31–42	60/40 hexane/EtOAc	Pale yellow solid
43–52	50/50 hexane/EtOAc	Pale yellow solid
53–60	45/55 hexane/EtOAc	Pale yellow solid
61–70	40/ 60 hexane/EtOAc	Pale yellow solid
71–81	35/65 hexane/EtOAc	Yellow solid

Table 1. Chromatographic fractions of ethyl acetate concentrate of *Bauhinia variegata.*

Compound II	Solvent system					
	30% HOAc	50% HOAc	60% HOAc	BAW*	Forestal#	PhOH+
	11.68	**35.52**	**55.38**	**24.24**	**67.74**	**51.66**

Table 2. R_f X 100 values of compound in paper chromatography. *BAW—n- butanol: acetic acid: water (4:1:5). #Forestal—Acetic acid: Conc HCl: H_2O (30:3:10). +PhOH—Phenol saturated with water (3:1).

3), 188.1 (C–4), 164.3 (C–5), 97.6 (C–6), 166.6 (C–7), 93.6 (C–8), 162.9 (C–9), 106.2 (C–10), 130.8 (C–1'), 128.8 (C–2'), 114.0 (C–3'), 159.6 (C–4'), 114.0 (C–5'), 128.8 (C–6'), 56.8 (OCH3), 56.1 (OCH3), and 55.2 (OCH3).

Animals and ethical approval

Male Sprague–Dawley rats (6–8 weeks old) were acquired for animal investigations from King Saud University's Experimental Surgery and Animal Lab in Riyadh, Saudi Arabia. All animal experiments adhered to the ARRIVE guidelines and were conducted in compliance with the U.K. Animals (Scientific Procedures) Act, 1986, as well as the EU Directive 2010/63/EU pertaining to animal experimentation. The care and maintenance of the experimental animals complied with the rules, ethical policies, and procedures sanctioned by the ethics committee of King Faisal University (Approval No: ETHICS2464). The rats were kept in polypropylene cages with conventional laboratory settings, including a 12-h light/dark cycle, a temperature of 25 °C, and a relative humidity of 60–70%, and all animals were acclimated for one week before the experiment began. Food and water were freely available to the animals.

Experimental design and animal grouping

This study was designed as a randomized, controlled, in vivo experiment with four parallel groups (n = 6 per group; total N = 24). The study included male Sprague–Dawley rats that were 6–8 weeks old and weighed between 200 and 250 g at the start of the experiment. Only animals that were healthy, free of clinical signs of disease, and exhibited normal behavior during the 7-day acclimatization period were included. Animals within each group had comparable baseline body weights to minimize bias due to metabolic or inflammatory responses. The animals were not previously exposed to experimental drugs, LPS, or surgical interventions. The animals were randomly assigned to the following groups using a computer-generated randomization method.

Control group (Vehicle-treated): Rats received 0.05% DMSO orally via gavage[20].

LPS group (Disease model): Rats received lipopolysaccharide (LPS) at 1 mg/kg body weight, intraperitoneally (i.p.), once daily for 4 weeks[21].

LPS + TMF group (Treatment group): Rats received LPS (1 mg/kg, i.p.) once daily for 4 weeks. Parallely, TMF (75 mg/kg, dissolved in 0.05% DMSO) was administered 4 h after LPS from Day 1 until the end of the 4-week study period.

TMF-alone group: Rats received TMF (75 mg/kg, orally) daily from Day 1 to the end of Week 4.

All treatments were administered via oral gavage using sterilized feeding needles under aseptic conditions. The dose and route of administration were selected based on previous studies demonstrating the bioactivity and tolerability of TMF in rodent models[18].

Sample collection and euthanasia

At the end of the 4-week experimental period, all the animals were anesthetized with intraperitoneal sodium pentobarbital (60 mg/kg, Sigma-Aldrich). Euthanasia was performed by transcardial perfusion with sterile 0.9% saline solution to minimize blood contamination of the tissues. Following perfusion, blood was collected via cardiac puncture for serum analysis. Tissue samples (jejunum and ileum) were rapidly excised, rinsed in ice-cold saline, and processed as follows:

- Histological analysis (fixed in 10% neutral-buffered formalin),
- Biochemical assays (flash frozen in liquid nitrogen and stored at – 80 °C),
- Molecular studies (tissue samples were frozen at – 80 °C until processing).

Examination of hepatic marker enzymes

Serum concentrations of ALT and AST were quantified with an ELISA reader (Bio-Tek Instruments, Inc., Winooski, VT, USA) at a wavelength of 505 nm. Blood samples obtained from the rats were subjected to centrifugation at 3000 × g for 10 min at 4 °C to isolate the serum. The supernatant was meticulously collected and preserved at – 80 °C for subsequent analysis. The activities of ALT and AST were measured according to the manufacturer's guidelines using commercially available assay kits.

Serum cytokines

Serum concentrations of TNF-α, IL-6, and IL-1β were measured using enzyme-linked immunosorbent assay (ELISA) kits from SE L. Biotec Co., Ltd. (Shanghai, China). Blood samples were obtained and centrifuged at 3,000 × g for 10 min at 4 °C to isolate the serum. The supernatant was meticulously collected and preserved at – 80 °C until analysis. ELISAs were conducted following the manufacturer's guidelines, and the absorbance was quantified using a microplate reader. Cytokine concentrations were quantified using standard curves derived from known quantities of recombinant cytokines.

Determination of serum diamine oxidase (DAO) activity

To assess intestinal mucosal integrity, serum diamine oxidase (DAO) activity was measured using a specialized commercial kit (Nanjing Jiancheng Institute of Bioengineering, Nanjing, China), following the manufacturer's recommended procedure. Briefly, blood samples were collected and centrifuged at 3,000 × g for 10 min at 4 °C to separate the serum. The resulting supernatant was carefully collected and stored at – 80 °C until further analysis. DAO activity in the serum was evaluated at a wavelength of 340 nm using a microplate reader, as specified by the kit instructions. DAO serves as a marker for intestinal barrier function, as increased serum levels typically indicate compromised mucosal integrity.

Determination of serum D-lactic acid (D-LA) concentration

Serum D-lactic acid (D-LA) concentration was determined to further evaluate intestinal permeability. Using a commercial detection kit (Nanjing Jiancheng Institute of Bioengineering, Nanjing, China), assays were conducted according to the manufacturer's protocol. Blood samples were centrifuged at 3,000 × g for 10 min at 4 °C to yield serum, which was then frozen at – 80 °C until analysis. For the D-LA assay, the absorbance was measured at 530 nm with a microplate reader. D-LA is considered a sensitive biomarker of intestinal barrier disruption, as elevated serum levels reflect increased intestinal permeability and bacterial translocation.

Assessment of oxidative stress markers

For oxidative stress evaluation, tissue homogenates were first prepared and centrifuged, with supernatants subjected to a panel of biochemical assays.

Malondialdehyde (MDA)

MDA levels, an indicator of lipid peroxidation, were quantified using the thiobarbituric acid reactive substances (TBARS) assay. This method involves reacting MDA with thiobarbituric acid to form a colored complex, the absorbance of which was measured at 532 nm. Elevated MDA levels suggest increased oxidative damage in tissues.

Superoxide dismutase (SOD) activity

SOD activity was assessed through its capacity to inhibit the reduction of nitroblue tetrazolium by superoxide anions. The decrease in absorbance corresponds to SOD enzyme activity, measured spectrophotometrically according to the manufacturer's instructions.

Catalase (CAT) activity

Catalase activity was determined by monitoring the rate of hydrogen peroxide (H_2O_2) breakdown. The decrease in absorbance at 240 nm over time served as an indicator of CAT enzymatic activity.

Glutathione (GSH) content

Tissue GSH content was measured using a specific colorimetric assay, where the intensity of color development reflects the concentration of GSH. The method involves a reaction with a chromogenic substrate, and absorbance is typically measured at a designated wavelength set by the kit protocol.

Total antioxidant capacity (T-AOC)

T-AOC was determined by evaluating the ability of the samples to counteract a standard oxidizing agent, resulting in a change in color intensity. Absorbance was recorded at 520 nm to reflect the overall antioxidant potential of the tissue sample. Higher T-AOC values suggest better antioxidative defense mechanisms.

For all assays, commercially available kits from Nanjing Jiancheng Bioengineering Institute were used, and procedures were carried out strictly according to the manufacturer's instructions.

Western blotting

Protease and phosphatase inhibitors added to RIPA buffer were used to isolate proteins from the ileum and jejunum. The protein concentrations were measured in a BCA assay. SDS-PAGE was used to separate identical quantities of protein, which were then transferred to PVDF membranes. After an hour of incubation at room temperature with 5% nonfat dry milk, the membranes were treated with primary antibodies targeting NF-κB, IL-1β, IL-6, and TNF-α overnight at 4 °C. Secondary antibodies conjugated to HRP were used to treat the

membranes after they had been cleaned. β-actin was used as the loading control for normalization, and protein bands were detected using an ECL detection method and quantified in Image Studio Lite software.

Histological analysis

Ileum and jejunum tissue samples were obtained, washed with cold PBS, and preserved in 10% neutral-buffered formalin for 24 h. The fixed tissues were subsequently dehydrated using a graded ethanol series, cleaned with xylene, and embedded in paraffin. Sections with a thickness of 5 µm were excised using a microtome and affixed to glass slides. The sections were stained with hematoxylin and eosin for histological assessment. Images of the stained sections for morphometric analysis were obtained using a light microscope with digital imaging equipment. Villus height (VH), measured from the tip to the base of the villus, and crypt depth (CD), measured from the base of the villus to the muscularis mucosa, were quantified using ImageJ software (National Institutes of Health, Bethesda, MD, USA). A minimum of 10 properly aligned villi and crypts were assessed per sample to guarantee precision. The villus height-to-crypt depth (VH/CD) ratio was computed as a metric of intestinal anatomy and functionality.

Immunohistochemistry

Sections from formalin-fixed, paraffin-embedded blocks were cut at a thickness of 5 µm using a microtome and affixed to glass slides. The slides were deparaffinized in xylene, rehydrated through a graded ethanol series, and rinsed with PBS. The sections were subjected to antigen retrieval by incubation in citrate buffer (pH 6.0) and subjected to heating in a microwave or pressure cooker for 15 min. Following cooling, endogenous peroxidase activity was inhibited via the addition of 3% H_2O_2 in methanol for 10 min at ambient temperature. Nonspecific binding was reduced by incubating the sections with 5% BSA for 30 min. The sections were subsequently treated overnight at 4 °C with a primary antibody targeting NF-κB (1:500). Following washing with PBS, the sections were incubated with a biotinylated secondary antibody for 45 min at ambient temperature and then treated with an HRP complex. Immunoreactivity was detected using DAB as the chromogen, resulting in brown staining.

Details of all the antibodies used for IHC and Western blotting were provided in supplementary file 1.

Statistical analysis

All the data are expressed as the means ± standard deviations. Statistical analyses were conducted using GraphPad Prism 10.1.2. Comparisons among groups were performed via one-way ANOVA followed by Tukey's post hoc analysis. A P value less than 0.05 was considered statistically significant. $*p < 0.05$ indicates a statistically significant difference between the LPS and control groups, whereas $@p < 0.05$ indicates a statistically significant difference between the LPS and LPS + TMF groups.

Results

Compound characterization

The substance was isolated from the ethyl acetate fraction of a 95% alcohol extract of the stem of *B. variegata*. It was obtained as a yellow amorphous powder with m.f. C18H18O5, m.p. 205 °C, and (M) + m/z 314 (EIMS). It produced a distinctive color response to flavonoids. Alcohol caused the chemical to crystallize into a yellow, amorphous powder. The chemical only displayed a shoulder for Band I at 320 nm and a high UV absorption maximum for Band II at 283 nm. This revealed the presence of a flavanone moiety within it, which was evidenced by the positive response of the compound to Shinoda's reagent.

There was no characteristic shift in Band II (major absorption peak) upon the addition of NaOMe, NaOAc, NaOAc/H_3BO_3, $AlCl_3$ or $AlCl_3$/HCl. These findings suggest that the A ring of the basic flavonoid skeleton lacks a hydroxyl group. The compound's 1H-NMR spectrum showed two A2 B2 patterns due to protons at C–3°, C–5∂, C–2∂, and C–6, respectively, with C–4∂ being an oxygenated substitution of ring B if flavanone 14 was present. Doublets in the aromatic region at δ 7.18 (J = 8.5 Hz) and δ 6.61 (J = 8.5 Hz), each integrating two portions, were detected. H-6 and H-8 of the A ring of the flavanone were identified as meta-linked one-proton doublets at δ 5.95 (J = 2.5 Hz) and δ 6.12 (J = 2.5 Hz), respectively[11,13].

The methoxyl group was identified by the single proton signals in the 1H-NMR spectra at 4.09, 3.90, and 3.74 ppm. The 13C-NMR spectrum of the molecule, which corresponds to the signals at δ 55.2, 56.1, and 56.8, further confirmed the presence of a methoxyl group. The absence of a free hydroxyl group at C–5 was demonstrated by the lack of a distinctive bathochromic shift upon the addition of AlCl3 and AlCl3/HCl. This was further supported by the lack of a signal at δ 12–14 ppm. Therefore, it was determined that a methoxyl group might replace C–5. Because the absence of shifts in λmax with shifting reagents suggested that the other two methoxyl groups were blocked, they may be positioned at C–7 and C–4° (normal oxygenated sites). Diagnostic RDA fragments at m/z A + 181 and B + 134, which are compatible with the presence of two methoxy groups in the A ring and one methoxy group in the B ring, respectively, were obtained from the EI-MS fragmentation of an [M +] ion at m/z 314. Therefore, the structure of the chemical was determined to be 5,7,4'-trimethoxyflavanone based on UV, 1H NMR, 13C NMR, and EIMS spectral studies (Fig. 1A–D).

Body weight changes

The final body weight data are depicted in Fig. 2A. Compared with the control, LPS significantly reduced the average body weight by 10%. Compared with the LPS group, TMF pretreatment increased the average daily gain under inflammatory conditions by 10%.

Hepatic marker enzymes (ALT and AST)

In the control group, alanine aminotransferase (ALT) and aspartate aminotransferase (AST) levels were within normal limits. LPS-treated animals showed a marked elevation in both ALT and AST, signifying hepatic injury

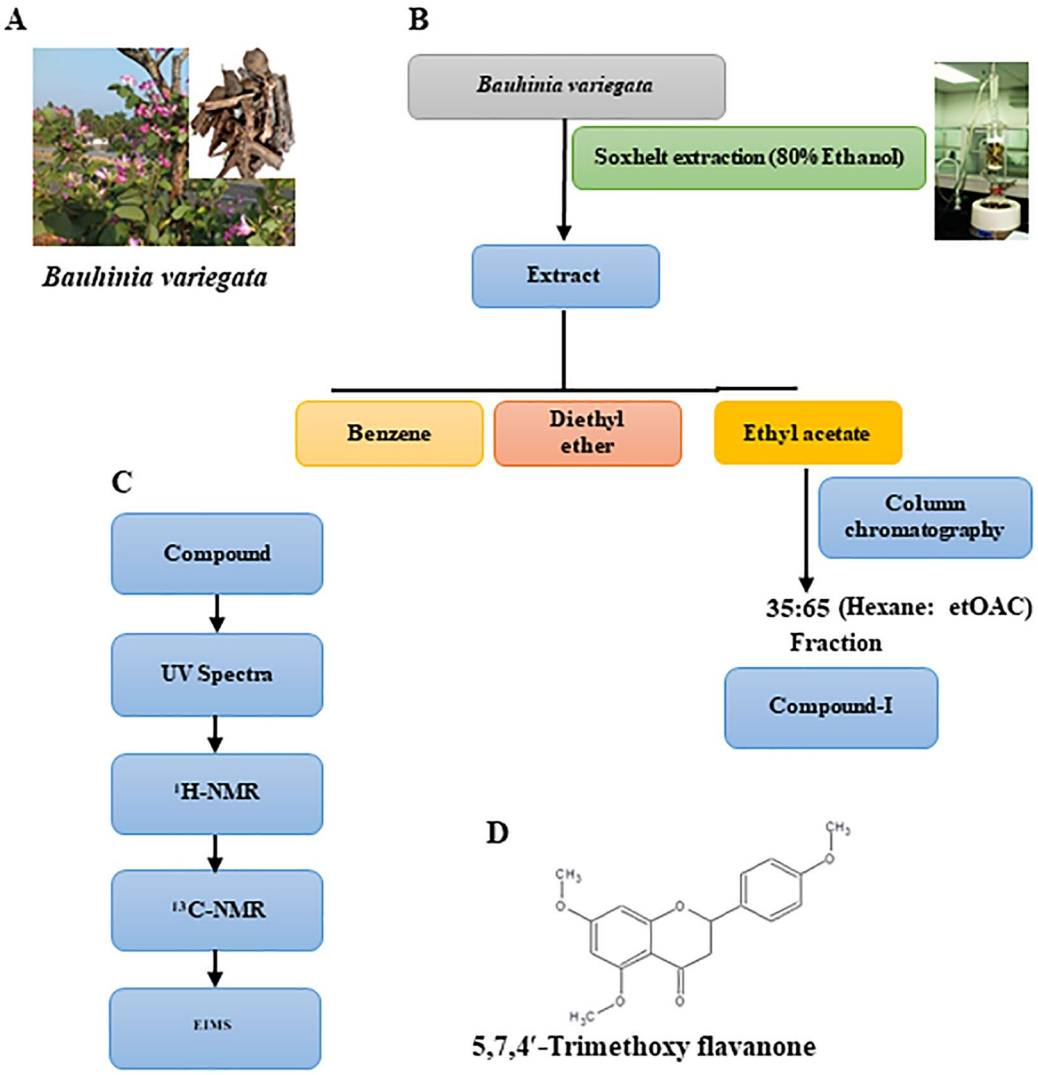


Fig. 1. Isolation, purification, and identification of TMF. (**A**). *Bauhinia variegata*. (**B**). Flowchart depicting the isolation of phytoconstituents. (**C**). Workflow for the characterization of Compound I. (**D**). Chemical structure of TMF.

and inflammation secondary to intestinal inflammation. TMF pretreatment significantly reduced the levels of these enzymes in the LPS + TMF group compared to the LPS-only group ($p < 0.05$), suggesting a hepatoprotective and anti-inflammatory effect. The TMF-only group exhibited no notable deviations from the control group, further supporting TMF's physiological safety (Fig. 2B).

Serum inflammatory cytokines (TNF-α, IL-6, IL-1β)

Serum concentrations of TNF-α, IL-6, and IL-1β were significantly elevated in the LPS group relative to controls, confirming heightened inflammation. TMF treatment in the LPS + TMF group significantly reduced these cytokine levels compared to the LPS group ($p < 0.05$), reflecting TMF's potent anti-inflammatory activity. No substantial differences were observed between the TMF-only and control groups, indicating a lack of pro-inflammatory effect with TMF alone (Fig. 2C–E).

Serum diamine oxidase (DAO) activity

Serum DAO activity was significantly decreased in the LPS-treated animals, indicating compromised intestinal mucosal integrity. TMF administration in the LPS + TMF group significantly restored DAO activity towards baseline levels compared to the LPS group ($p < 0.05$), signifying TMF's role in preserving gut barrier function. DAO levels in the TMF-only group did not differ from those in the control group (Fig. 2F).

Serum D-lactic acid (D-LA) levels

D-LA levels were significantly elevated in the LPS group, revealing enhanced gut permeability and barrier dysfunction. In contrast, the LPS + TMF group showed a marked reduction in D-LA concentrations compared

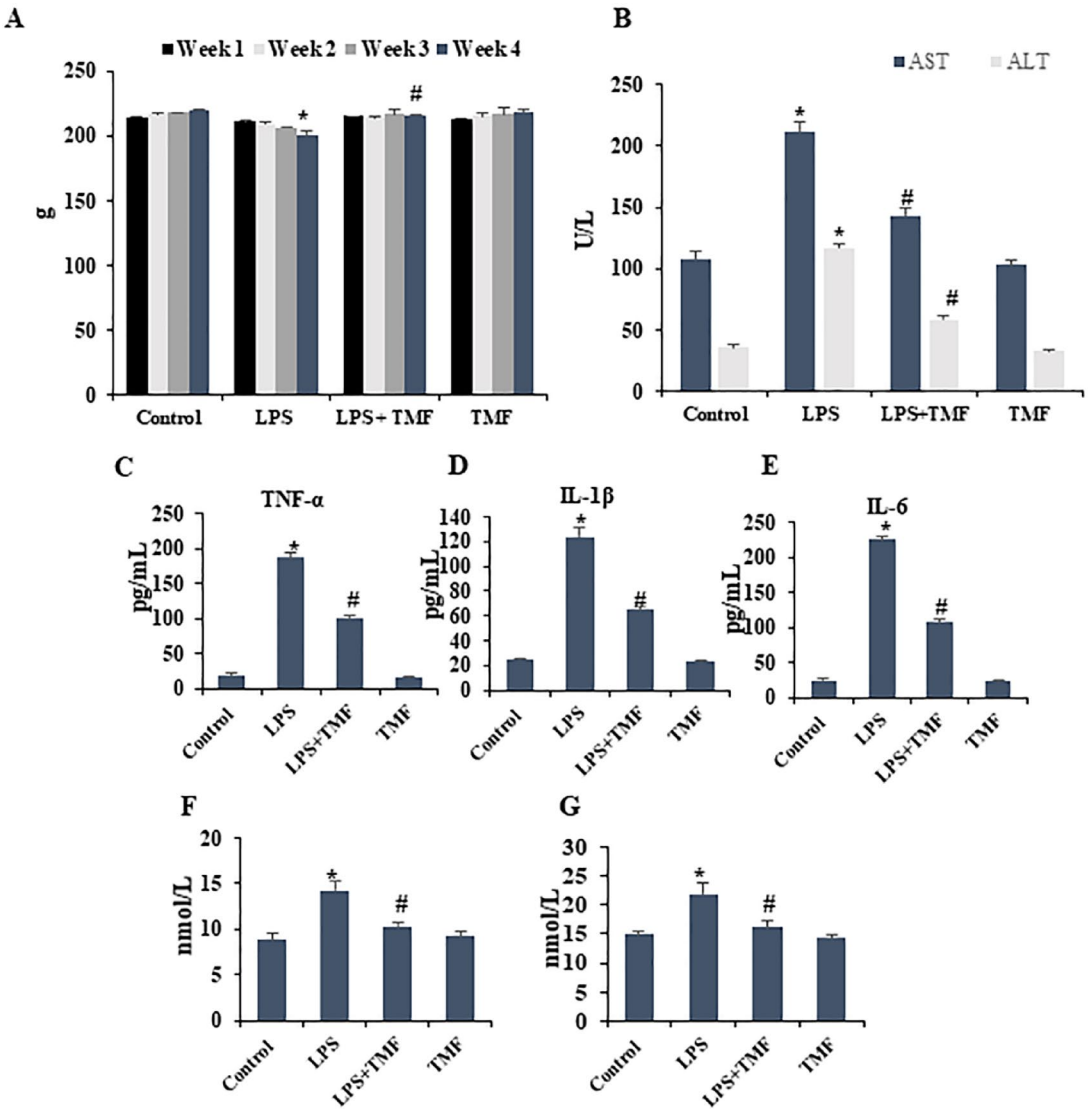


Fig. 2. Effects of TMF on the levels of serum markers of LPS-induced intestinal inflammation, as well as diamine oxidase and D-lactate acid. (**A**). The graph indicates the average body weight (in %) of the experimental animals at the end of the treatment. (**B**). AST (U/L) and ALT (U/L) markers indicate liver injury, which was assessed in all four groups (**C**–**E**). DAO levels (**F**). D-LA levels (**G**). When n = 6, $*p < 0.05$ indicates a significant difference between the LPS and control groups. Likewise, $@p < 0.05$ indicates a significant difference between the LPS and LPS + TMF groups.

to the LPS group ($p < 0.05$), consistent with improved intestinal barrier integrity. D-LA values in the TMF-only group remained similar to those in controls (Fig. 2G).

Oxidative stress markers (MDA, SOD, CAT, GSH, T-AOC)

In both jejunal and ileal tissues, LPS exposure led to a significant increase in Malondialdehyde (MDA) (Fig. 3Aa and Ba), superoxide dismutase (SOD) (Fig. 3Ab and Bb), catalase (CAT) (Fig. 3Ac and Bc), glutathione (GSH) (Fig. 3Ad and Bd), and total antioxidant capacity (T-AOC) (Fig. 3Ae and Be) ($p < 0.05$). TMF treatment notably decreased MDA levels and restored SOD, CAT, GSH, and T-AOC activities in the LPS + TMF group ($p < 0.05$), indicating enhanced antioxidative protection and reduced oxidative damage. There were no significant alterations in these biomarkers in the TMF-only group compared to controls.

Western blot: NF-κB and cytokines in intestinal tissue

Compared with those in the control group, Western blot analysis revealed that the protein expression levels of NF-κB, TNF-α, IL-1β and IL-6 in the LPS-treated group ($p < 0.05$) revealed that LPS-induced intestinal inflammation significantly activated the NF-κB signaling pathway in the jejunum (Fig. 4) and ileum (Fig. 5). These inflammatory markers indicate that LPS provoked a strong inflammatory response. TMF treatment significantly reduced the activation of the NF-κB pathway in the LPS + TMF group. Compared with those in the

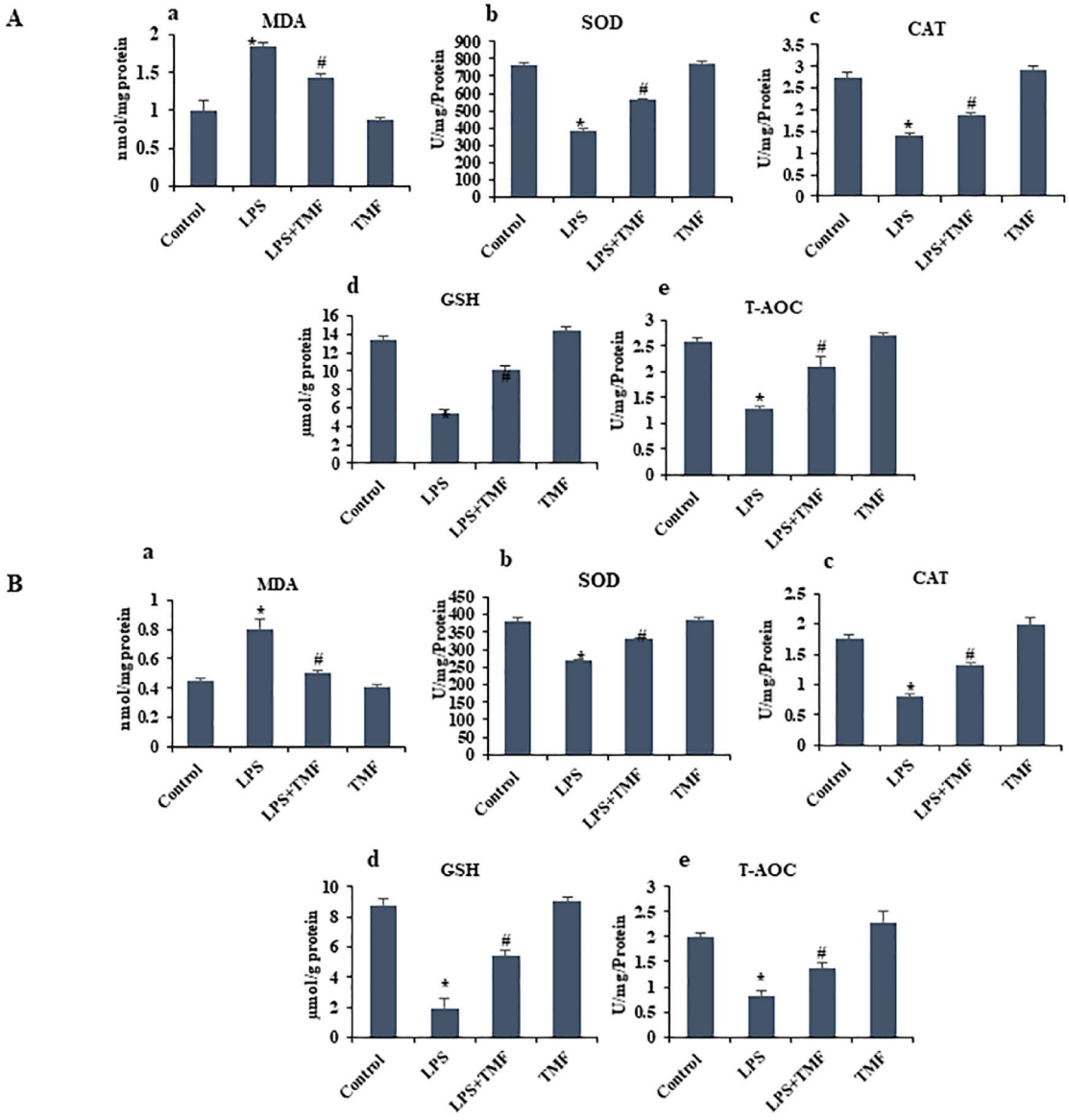


Fig. 3. Impact of TMF on the oxidant status of the small intestine in rats subjected to LPS-induced intestinal inflammation. (**A**) Jejunum; (**B**) ileum. MDA: malondialdehyde (nmol/mg/protein) (Aa and Ba); SOD: superoxide dismutase (U/mg/protein) (Ab and Bb); CAT: catalase (U/mg/protein) (Ac and Bc); GSH: glutathione (μmol/g/protein) (Ad and Bd); T-AOC: total antioxidant capacity (U/mg/protein) (Ae and Be). When n = 6, $*p < 0.05$ indicates a significant difference between the LPS and control groups. Likewise, $@p < 0.05$ indicates a significant difference between the LPS and LPS + TMF groups.

LPS group, the protein concentrations of NF-κB, TNF-α, IL-6, and IL-1β were substantially lower in the jejunal and ileal tissues of patients in the LPS + TMF group ($p < 0.05$). TMF efficiently reduces intestinal inflammation caused by LPS, as evidenced by the suppression of proinflammatory cytokines and NF-κB. Compared with the control group, the TMF-only group presented no apparent differences in NF-κB, TNF-α, IL-6, or IL-1β levels, indicating that TMF alone did not cause any inflammatory response in a typical situation. These findings show that TMF has potent anti-inflammatory effects on the ileum and jejunum by significantly inhibiting the NF-κB signaling pathway and reducing the expression of proinflammatory cytokines in the context of LPS-induced intestinal inflammation.

Immunohistochemical staining for NF-κB

Immunohistochemical analysis of NF-κB in jejunal (6A) and ileal (6B) tissue samples revealed pronounced nuclear localization and expression of NF-κB in the LPS-treated cohort, indicating robust activation of the NF-κB signaling pathway due to LPS-induced intestinal inflammation. The staining was notably pronounced in the epithelial cells of the villi and crypts, as well as in the infiltrating inflammatory cells, in contrast to the control group, which exhibited negligible NF-κB expression (Fig. 6A and B). In the LPS + TMF group, NF-κB expression

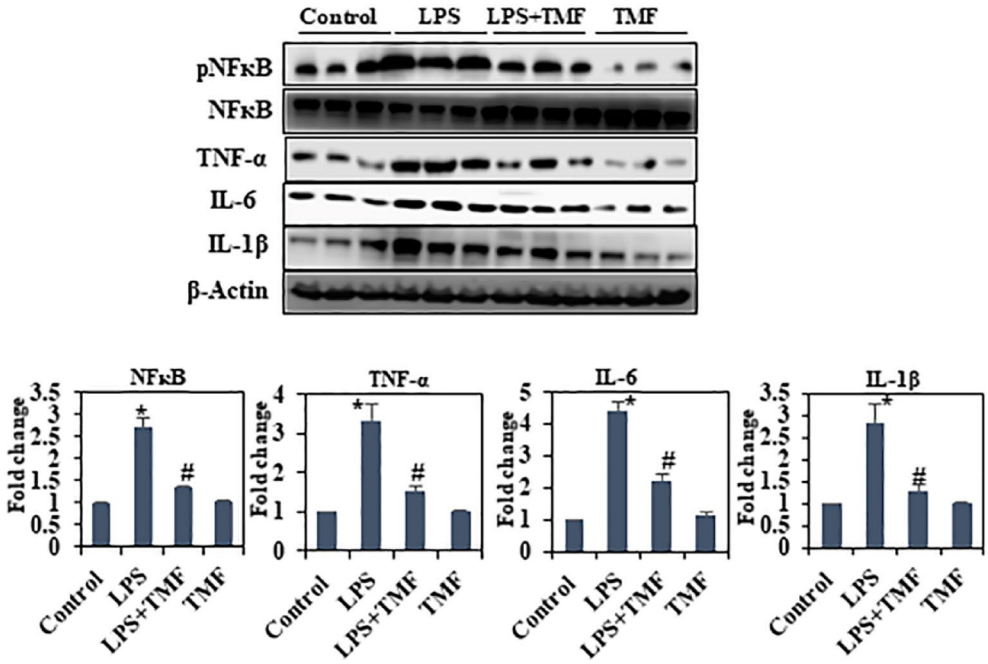


Fig. 4. Effect of TMF on NFκB signaling pathways in the jejunum. Western blot analysis of NFκB, IL-6, TNF-α and IL-1β in the jejunum. When n = 6, $^{*}p < 0.05$ indicates a significant difference between the LPS and control groups. Likewise, @p < 0.05 indicates a significant difference between the LPS and LPS + TMF groups.

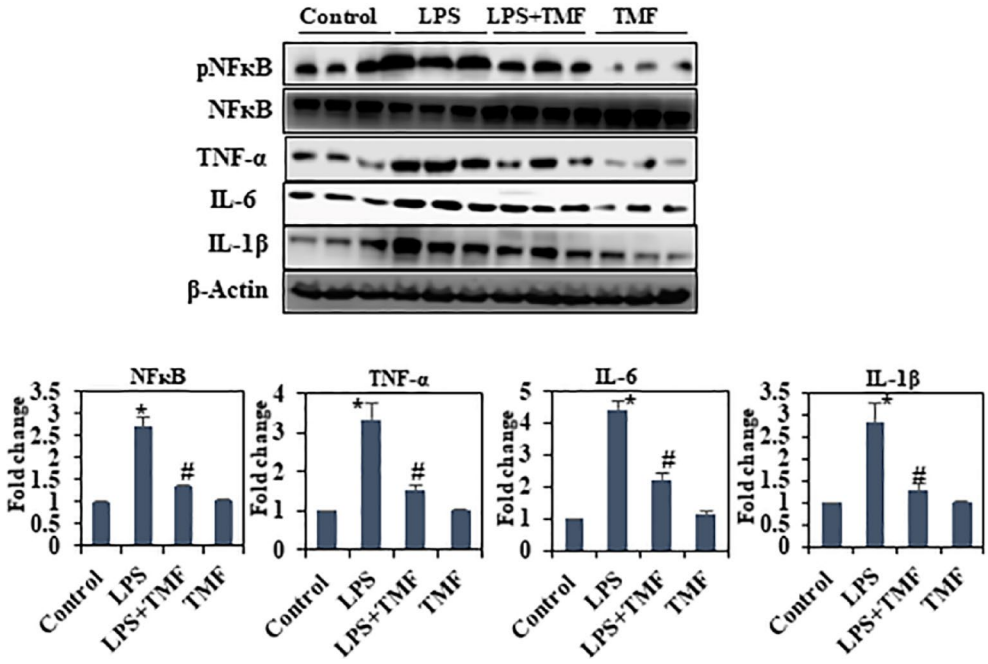


Fig. 5. Effect of TMF on the NFκB signaling pathway in the ileum. Western blot analysis of NFκB, IL-6, TNF-α and IL-1β in the ileum. When n = 6, $^{*}p < 0.05$ indicates a significant difference between the LPS and control groups. Likewise, $@p < 0.05$ indicates a significant difference between the LPS and LPS + TMF groups.

levels were markedly diminished in both jejunal and ileal tissues. Nuclear staining of NF-κB was significantly reduced, demonstrating that TMF effectively suppressed the activation and translocation of NF-κB into the nucleus. The overall staining intensity and number of positively stained cells were markedly lower than those in the LPS group ($p < 0.001$). The flavanone-alone group presented NF-κB expression levels comparable to those of the control group, with negligible nuclear staining, indicating that TMF does not activate NF-κB under normal

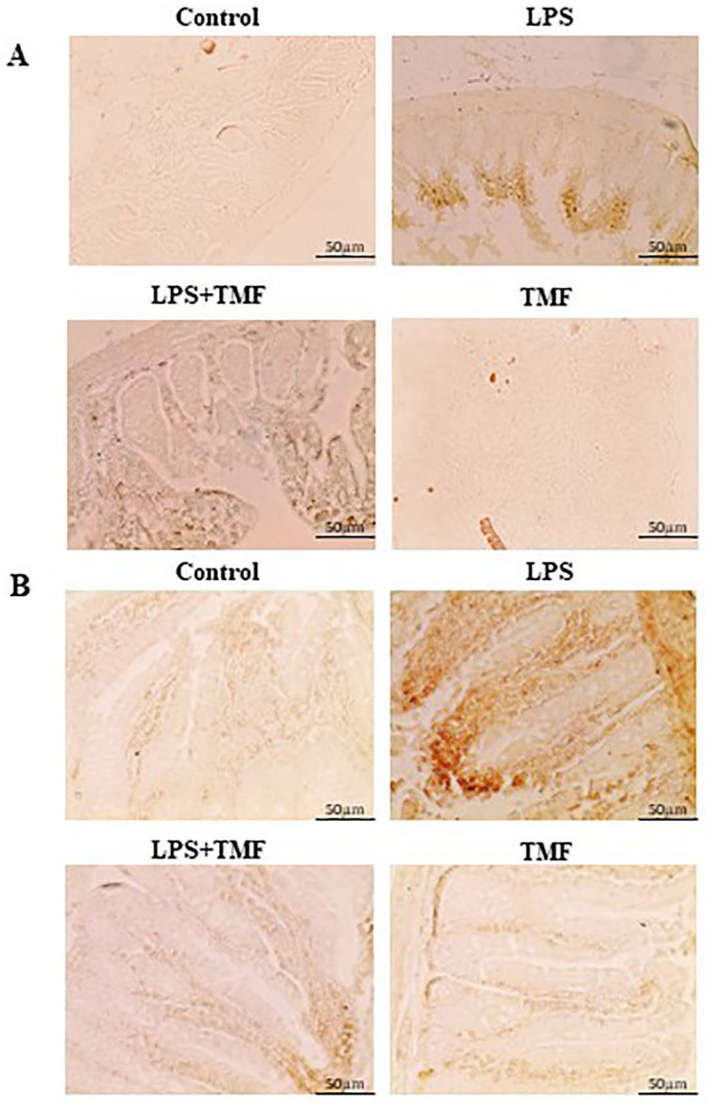


Fig. 6. IHC staining of NFκB in the (**A**) jejunum and (**B**) ileum of experimental rats. Scale bar (50 µm). Magnification 40×.

Solvent/shift reagents	λ_{max} (nm)
MeOH	283, 320
+ NaOMe	283, 330
+ $AlCl_3$	283, 315
+ $AlCl_3$ + HCl	282, 315
+ NaOAc	283, 315, 372
+ NaOAc + H_3BO_3	283, 315, 372

Table 3. λ_{max} values of compound.

physiological conditions. These results indicate that TMF markedly inhibits NF-κB activation in response to LPS-induced intestinal inflammation, as shown by the reduced nuclear localization and expression of NF-κB in jejunal and ileal tissues (Table 3).

Table 4 shows significant p-values ($p < 0.001$), indicating that there are statistically significant differences in NF-κB staining among the groups (Control, LPS, LPS + TMF, and TMF) in both Jejunum and Ileum. To assess differences among treatment groups, a non-parametric Kruskal–Wallis test was followed by post-hoc pairwise comparisons using Dunn's test with Bonferroni correction for multiple testing. In Jejunum, pairwise comparisons between the LPS-treated group show significantly increased measured values compared to the Control ($p < 0.001$). The LPS + TMF group also showed significantly higher values compared to the Control

δ H (ppm)	Signal assignment
7.18	2H, d, (J = 8.5 Hz) 2′, 6′ of ring B
6.61	2H, d, (J = 8.5 Hz) 3′, 5′ of ring B
6.12	1H, d, (J = 2.5 Hz) H-8 of ring A
5.95	1H, d, (J = 2.5 Hz) H-6 of ring A
5.26	1H, dd, (J = 13.0, 3.0 Hz) H-2 of ring C
4.09	3H, s Methoxyl Proton
3.90	3H, s Methoxyl Proton
3.74	3H, s Methoxyl Proton
2.89	1H, dd; (J = 17.0, 3.0 Hz) H-3 of ring C
2.81	1H, dd; (J = 17.0, 3.0 Hz) H-3 of ring C

Table 4. ^{1}H-Data of Compound in $CDCl_3$.

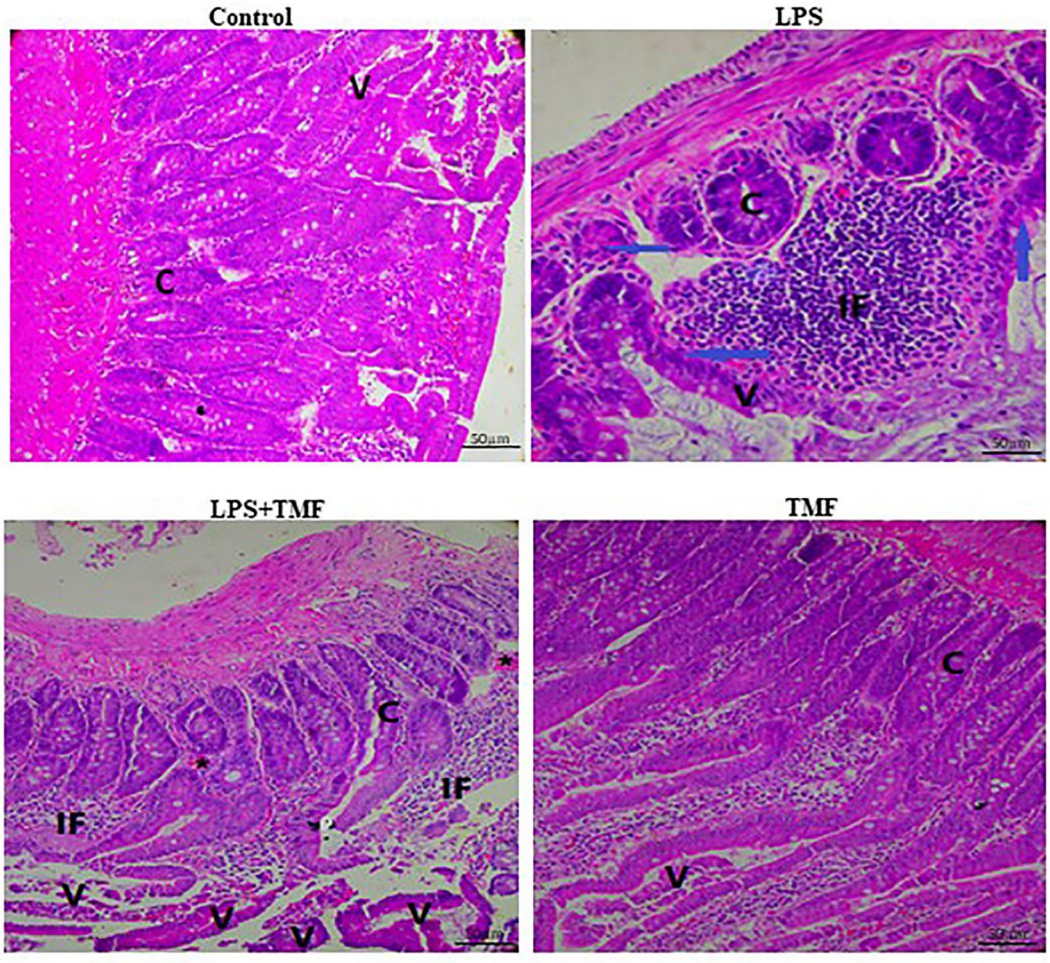


Fig. 7. Impact of TMF on jejunum morphology in rats subjected to LPS-induced intestinal inflammation. Histopathological examination of the jejunum (H&E staining). Magnification 40×. C-crypts of lieberkuhn; V-villi; IF-inflammatory cell infiltration; black arrows indicate destruction of crypts. *; congested blood vessels.

($p < 0.001$). No significant difference was found between Control and TMF alone ($p = 1.00$). LPS + TMF treatment significantly differed from LPS alone ($p < 0.001$), suggesting a modulatory effect of TMF. Both LPS and LPS + TMF differed significantly from TMF ($p < 0.001$). These findings indicate that LPS induces a measurable response that is attenuated, but not normalized, by TMF co-treatment. Similarly, in the ileum (Fig. 6 B), both LPS and LPS + TMF groups significantly differed from Control ($p < 0.001$). The TMF group alone was not significantly different from Control ($p = 1.00$). While LPS and LPS + TMF groups showed significant differences. To conclude it is evident that TMF alone does not alter baseline levels but significantly modulates the LPS-induced response.

Histological changes observed in the jejunum in control vs treated rats

The jejunum of the control animal displayed a normal histological structure, featuring well-organized, intact villi (V) and structurally conserved crypts (C) (Fig. 7). The epithelial lining was transparent and intact. After

treatment with LPS, the jejunum of the rats that were administered LPS exhibited significant inflammatory damage, encompassing severe inflammatory cell infiltration (IF), abnormal glandular formations, and crypt destruction (C). The villi displayed a loss of their distinctive columnar cell architecture, along with ulceration and mucosal erosion (V). Supplementary pathological alterations included vascular congestion, necrosis, and bleeding within the villi and crypts (blue arrows). The jejuna of the rats treated with TMF exhibited regenerative mucosa characterized by minor crypt distortion and considerable inflammatory cell infiltration in the lamina propria, suggesting partial healing. In the TMF-only-treated rats, the jejunum displayed a preserved mucosal structure, with little inflammatory cell infiltration in the lamina propria. The villi and crypts were well preserved in both dimensions and integrity, closely mirroring those of the control group.

Histological changes observed in the ileum in control vs treated rats

The control group displayed a typical histological architecture in the ileum, characterized by well-structured villi (V) and preserved crypts (C) (Fig. 8). The epithelial lining and lamina propria exhibited no evidence of inflammation or structural anomalies. Conversely, rats administered LPS exhibited notable architectural disruptions. The villous structures were irregular, exhibiting shorter and atrophic villi. The lamina propria exhibited a significant increase in inflammatory cell infiltration (IF). Furthermore, mucosal ulcers, crypt distortion, and bleeding were apparent. Additionally, blood vessels were engorged, and the crypts displayed irregularities, including branching, dilatation, and atrophy (black arrows). The coadministration of TMF conferred protective benefits against damage generated by LPS. The villous architecture was partially reinstated, whereas the mucosal layer, encompassing the epithelium, remained predominantly unaltered. Despite the presence of submucosal edema and modest inflammatory cell infiltration, the levels of overall structural integrity of the villi and crypts were markedly greater than those in the LPS-treated group. The rats that were administered TMF only presented a normal ileal histology, closely mirroring that of the control group. The villi (V) and crypts (C) exhibited excellent preservation in both dimensions and integrity, with no indications of

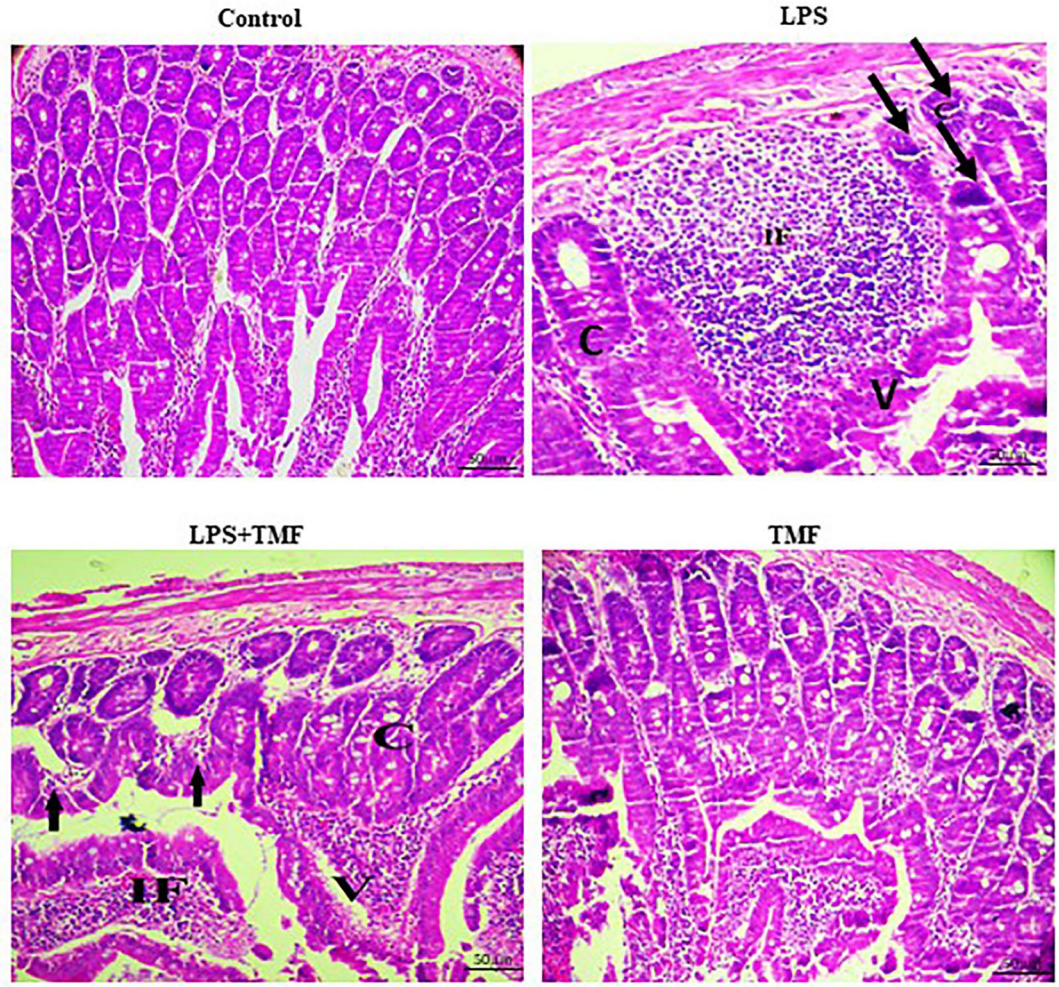


Fig. 8. Impact of TMF on ileum morphology in rats subjected to LPS-induced intestinal inflammation. Histopathological examination of the ileum (H&E staining). Magnification 40×. C-crypts of Luberkhun; V-villi; IF-inflammatory cell infiltration; blue arrows indicate destruction of crypts.

C	C–2	C–3	C–4	C–5	C–6	C–7	C–8	C–9	C–10
ppm	79.8	45.3	188.1	164.3	97.6	166.6	93.6	162.9	106.2

C	C–1′	C–2′	C–3′	C–4′	C–5′	C–6′	OCH_3	OCH_3	OCH_3
ppm	130.8	128.8	114.0	159.6	114.0	128.8	56.8	56.1	55.2

Table 5. 13C-NMR data compound in CDCl3.

	Control	LPS	LPS + TMF	TMF
Jejunum				
VH (μm)	408.62 ± 3.23	271 ± 5.25*	383 ± 4.19#	415.65 ± 7.5
CD (μm)	72.45 ± 4.24	60.20 ± 8.39*	68.93 ± 4.04#	75.32 ± 4.12
VH/CD (μm)	5.64 ± 0.75	4.50 ± 0.62	5.56 ± 1.03	5.51 ± 1.83
Ileum				
VH (μm)	382.26 ± 4.02	354.72 ± 16.38*	371.1 ± 12.32#	387.71 ± 10.46
CD (μm)	91.63 ± 9.41	82.33 ± 2.93*	87.46 ± 5.23#	91.41 ± 3.31
VH/CD (μm)	4.17 ± 0.42	4.30 ± 5.59	4.24 ± 2.35	4.24 ± 3.15

Table 6. Effects of TMF on intestinal mucosal morphology of Sprague Dawley rats in LPS induced inflammation. When (n = 6), *P < 0.05 indicates significant differences between the LPS group and the control group. Likewise, @ P < 0.05 indicates significant differences between the LPS group and the LPS + TMF group.

inflammatory cell infiltration or structural anomalies. The mucosa remained unblemished, further illustrating the protective function of TMF.

Effects of TMF on small intestine parameters

Analysis of the jejunum revealed notable differences in the villus height (VH), crypt depth (CD), and the VH/CD ratio among the various groups (Table 3). Compared with the control group (VH: 271 ± 5.25, CD: 60.20 ± 8.39), the LPS-treated group (VH: 408.62 ± 3.23, CD: 72.45 ± 4.24) presented significant reductions in villus height and crypt depth, suggesting inflammation-related structural damage. The LPS + TMF group exhibited significant recovery in both VH (383 ± 4.19) and CD (68.93 ± 4.12). The VH/CD ratio exhibited a comparable pattern, with the LPS group presenting the lowest value (4.5 ± 0.62), which significantly improved in the LPS + TMF group (5.56 ± 1.03). Table 5. Assessment of the ileum revealed changes in the villus height (VH), crypt depth (CD), and VH/CD ratio. Compared with the control group (VH: 382.26 ± 4.02, CD: 91.63 ± 8.41), the LPS group presented reductions in VH (354.72 ± 16.38) and CD (82.33 ± 2.93). Treatment with TMF improved these parameters in the LPS + TMF group (VH: 371.10 ± 12.32, CD: 87.46 ± 5.23). The TMF-only group presented marginally elevated values, indicating the protective potential of TMF. The VH/CD ratios were similar among the groups, with slight variations noted (Table 6).

Discussion

In the context of intestinal inflammation, particularly within the jejunum and ileum, the protective properties of flavanones are particularly vital. The jejunum and ileum are the principal locations for nutrient absorption in the small intestine and are crucial for preserving intestinal integrity, regulating immunity, and ensuring barrier function[22]. Inflammatory conditions, such as those triggered by LPS, can cause substantial disruption of the mucosal barrier, leading to villus atrophy, crypt hyperplasia, increased intestinal permeability, and immune cell infiltration. Inflammatory reactions are pivotal to the development of numerous gastrointestinal disorders, such as inflammatory bowel disease (IBD), Crohn's disease, and ulcerative colitis[23].

Flavonoids, which encompass various plant secondary metabolites, have been extensively researched for their significant anti-inflammatory, antioxidant, anticancer, and chemopreventive effects[24–26]. Among these, 5,7,4'-trimethoxyflavanone, a type of flavonoid, has attracted interest for its ability to regulate inflammatory pathways and safeguard against tissue damage. Flavonoids have demonstrated potential in alleviating many forms of inflammation, especially in the gastrointestinal tract, by reducing the activation of proinflammatory cytokines and transcription factors, including NF-κB, TNF-α, IL-6, and IL-1β[27,28].

LPS treatment commonly reduces animal body weight for numerous reasons. Inflammatory cytokines generated in response to LPS create anorexia, which reduces food intake and energy balance[29,30]. During the inflammatory response, the body increases energy consumption, and catabolic processes are activated to meet these energy needs, especially when the glucose stores are insufficient. This results in proteolysis and lipolysis to fuel immune functions and tissue repair[31,32]. Compared with control rats, LPS-treated rats lose weight faster because of lower intake and increased catabolism, a sign of systemic inflammation. Studies have shown that flavonoids can slow weight loss by reducing inflammation and metabolic effects[33,34]. To maintain metabolic health and prevent the negative consequences of systemic inflammatory responses, inflammation must be controlled. In this experimental study, TMF significantly reduced weight loss in experimental rats treated with these flavonoids compared with that in the LPS-treated group. TMF may lower the systemic inflammatory

response and sustain energy balance in animals by maintaining metabolic stability during the inflammatory process because of its anti-inflammatory and antioxidant characteristics.

LPS causes strong gastrointestinal inflammation, especially in the jejunum and ileum. The NF-κB signaling system is crucial for initiating and sustaining inflammation[35,36]. Within the nucleus, NF-κB associates with distinct DNA sequences known as κB sites, which are located in the promoter regions of proinflammatory genes. The transcription of several genes linked to inflammation, including cytokines such as TNF-α, IL-6, and IL-1β, is initiated by NF-κB. These inflammatory mediators enhance the immune response and attract additional immune cells to the site of inflammation, exacerbating intestinal tissue damage.

Our study revealed that LPS stimulation markedly elevated the serum concentrations of TNF-α, IL-6, and IL-1β. We observed the same phenomenon when the tissue concentrations of TNF-α, IL-6, and IL-1β were assessed. This study demonstrated that TMF markedly decreased proinflammatory cytokine production by inhibiting NF-κB in the jejunum and ileum of rats. These results support those of previous studies, which reported lower NF-κB production following treatment with substances such as the citrus flavonoid naringenin[37,38]. Owing to the inhibition of NF-κB translocation, the levels of the proinflammatory cytokines TNF-α, IL-6, and IL-1β decreased following pretreatment with TMF, indicating the downregulation of IL-1β and TNF-α. These data corroborate the anti-inflammatory properties of TMF. Our study also corroborates the findings of previous studies, where flavanone has been reported to inhibit inflammation via the suppression of inflammatory cytokines in RAW 264.7 cells[39].

Elevated serum levels of DAO and D-LA are related to intestinal dysfunction. Concurrent with the above-reported findings, serum D-LA and DAO levels were considerably reduced following dietary flavanone supplementation[40]. Likewise, Luo et al. (2023) reported that dietary flavanone supplementation reduced serum DAO activity[41]. These findings suggest that dietary TMF supplementation may effectively mitigate the intestinal barrier damage caused by LPS. LPS-induced tissue damage is characterized by an imbalance between oxidative and antioxidative components, resulting in excessive free radical generation and a reduction in antioxidants[42]. The concentrations of MDA, SOD, CAT, GSH, and T-AOC are critical indicators for evaluating oxidative damage in tissues caused by free radicals[43].

Oxidative stress is caused by an imbalance between available antioxidants and reactive oxygen species. Both in vitro and in vivo, flavanones have shown antioxidant potential[44,45]. The liver, spleen, and kidneys of rats may experience less oxidative damage from heat stress if the rats consume dietary flavonoid supplements[46]. In this study, LPS decreased ileal mucosal GSH activity and jejunal mucosal CAT, GSH, and T-AOC activities while increasing mucosal MDA levels in the ileum and jejunum. MDA was used as a marker for oxidative stress; as expected, dietary TMF supplementation increased CAT and T-AOC activities in the duodenum, T-AOC activity in the jejunum, and GSH activity in the ileum mucosa while decreasing mucosal MDA levels in the ileum and jejunum. The reduced MDA levels and the elevated activities of T-AOC, GSH, and CAT in the small intestine indicated an improved antioxidant capability. These results indicate that dietary TMF supplementation may mitigate oxidative damage to the small intestinal mucosa caused by heat stress.

The present study demonstrated that TMF effectively inhibits NF-κB activation in LPS-induced intestinal injury, but the precise mechanism through which TMF exerts this effect remains to be fully elucidated. Given that many flavonoids exert their anti-inflammatory effects not only by directly targeting NF-κB but also through upstream regulatory pathways, such as the PI3K/AKT and MAPK pathways, it is plausible that TMF follows a similar mechanism. Previous studies on structurally related flavonoids have shown that they can modulate oxidative stress and cytokine production, thereby indirectly suppressing NF-κB activation[47]. However, our study focused primarily on the overall impact of TMF on NF-κB signaling rather than its direct molecular interactions with pathway components. Future studies employing pathway-specific inhibitors or molecular docking approaches could help determine whether TMF interacts directly with NF-κB subunits or modulates its activity via upstream regulators (Fig. 9).

Histological investigation of the jejunum and ileum in the LPS-treated groups revealed significant tissue damage, as evidenced by the shortening and blunting of villi, elongation of crypts, and pronounced infiltration of inflammatory cells into the mucosa and submucosa. These histological markers indicate an inflammatory milieu that alters the normal structure of the intestinal epithelium. Furthermore, the identified tissue damage corresponds with standard LPS-induced dysregulation, including oxidative stress, increased intestinal permeability, and subsequent bacterial translocation, all of which enhance the inflammatory environment. The preventive effects of TMF are due to its established anti-inflammatory and antioxidant capabilities. TMF is a flavonoid recognized for its ability to inhibit the NF-κB pathway, a key regulator of proinflammatory cytokines, including TNF-α, IL-6, and IL-1β. The histological enhancements observed in the TMF-treated groups aligned with the downregulation of inflammatory mediators, as indicated by decreased immune cell infiltration and maintenance of the mucosal barrier. Moreover, TMF may augment the antioxidant defense mechanism in intestinal tissues, thereby diminishing oxidative stress, a principal factor in tissue damage during LPS-induced intestinal inflammation. TMF alleviates oxidative damage to the intestinal epithelium, which is otherwise intensified by LPS, by scavenging ROS and upregulating endogenous antioxidant enzymes.

The histology data indicate that TMF has a substantial protective effect on the jejunum and ileum during LPS-induced intestinal inflammation. TMF has potential as a therapeutic agent for regulating intestinal inflammation by preserving the villus architecture, diminishing inflammatory cell infiltration, and sustaining mucosal integrity. A limitation of this study is that it does not extensively examine the molecular mechanisms underlying TMF's effects, particularly its role in modulating inflammatory signaling pathways, which warrants further investigation to fully understand its therapeutic potential in conditions such as IBD and other gastrointestinal inflammatory diseases.

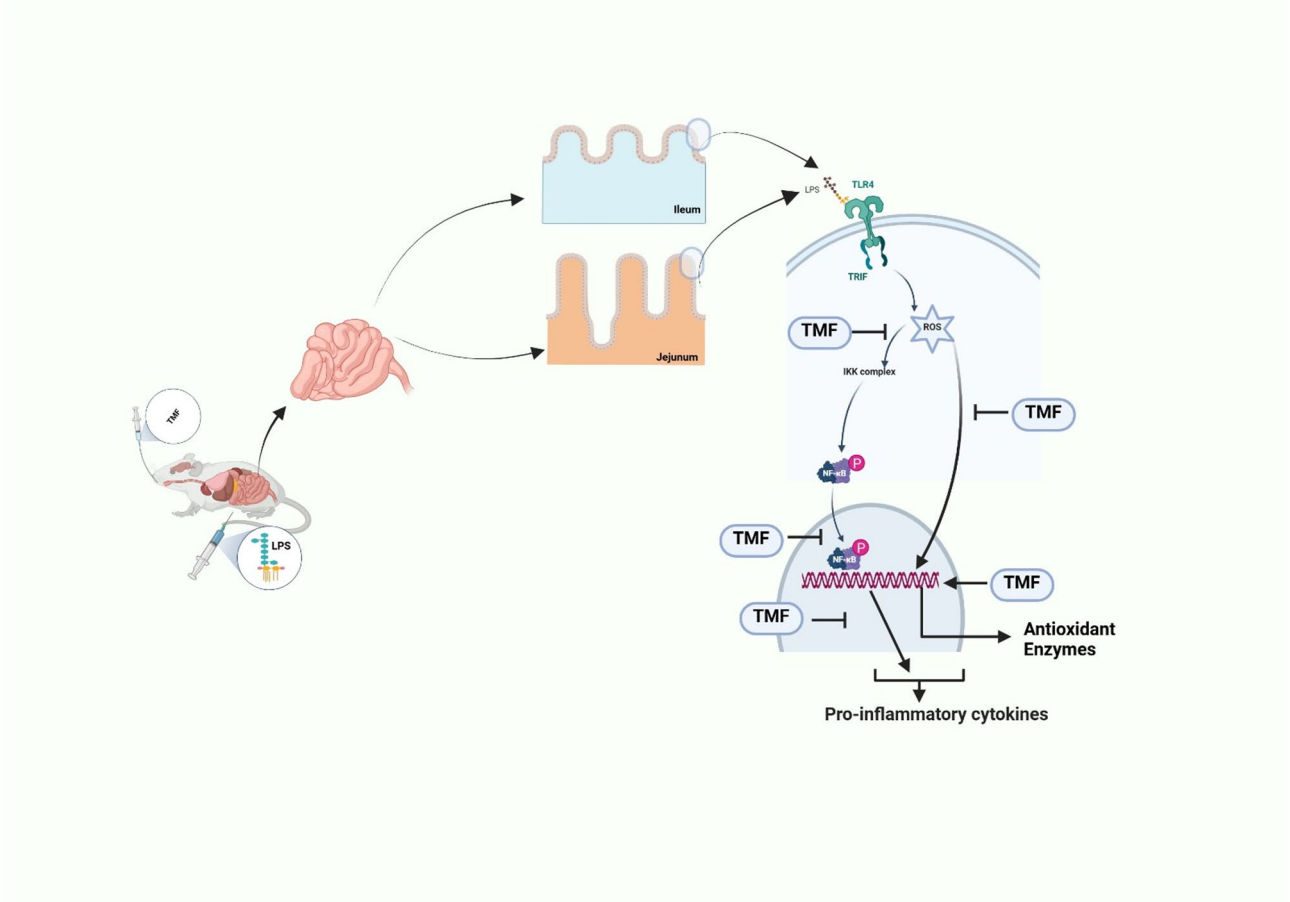


Fig. 9. Mechanistic diagram summarizing the proposed mode of action of TMF, illustrating its potential interaction with NF-κB either directly or via upstream regulators.

Conclusion

The findings of this study demonstrate that TMF effectively protects against LPS-induced inflammation in the jejunum and ileum. Treatment with TMF preserved the normal histological architecture of the intestinal tissue by reducing villus shrinkage, crypt overgrowth, and infiltration of inflammatory cells, highlighting its promise as a potent anti-inflammatory agent. These observations align with TMF's known inhibitory effects on proinflammatory signaling pathways like NF-κB, as well as its role in enhancing the body's natural antioxidant defenses. Consequently, TMF shows promise as a therapeutic option for conditions characterized by intestinal inflammation, such as inflammatory bowel disease, where preserving mucosal health is crucial for favorable clinical outcomes.

Future studies should focus on elucidating the precise mechanisms by which TMF functions as a strong anti-inflammatory and antioxidant agent, particularly in the context of chronic inflammation and oxidative stress. Investigating TMF's influence on additional inflammatory pathways, such as MAPK and PI3K/AKT, will be important for understanding its role in maintaining intestinal homeostasis during prolonged treatment. Moreover, evaluating TMF in chemically induced colitis and autoimmune-driven IBD models could provide valuable insights into its broader therapeutic applications. To advance clinical development, pharmacokinetic studies are also needed to establish the optimal dosing and bioavailability of TMF for effective use in patients. Finally, clinical trials on the efficacy and safety of TMF in humans with gastrointestinal inflammation will help translate preclinical discoveries into therapeutic realities.

Data availability

All materials are available from the corresponding author.

Received: 13 August 2025; Accepted: 30 October 2025
Published online: 28 November 2025

References

1. AlZahrani, A. M. et al. Protective effect of 5, 4'-dihydroxy-6, 8-dimethoxy7-O-rhamnosylflavone from Indigofera aspalathoides Vahl on lipopolysaccharide-induced intestinal injury in mice. *Inflammopharmacology* **32**, 3537–3551 (2024).

2. Yang, Y., Li, R., Hui, J., Li, L. & Zheng, X. β-Carotene attenuates LPS-induced rat intestinal inflammation via modulating autophagy and regulating the JAK2/STAT3 and JNK/p38 MAPK signaling pathways. *J. Food Biochem.* **45**, e13544 (2021).
3. Li, X. et al. Oligosaccharides isolated from *Rehmannia glutinosa* protect LPS-induced intestinal inflammation and barrier injury in mice. *Front. Nutr.* **10**, 1139006 (2023).
4. He, Y., Wang, D., Liu, K., Deng, S. & Liu, Y. Sodium humate alleviates LPS-induced intestinal barrier injury by improving intestinal immune function and regulating gut microbiota. *Mol. Immunol.* **161**, 61–73 (2023).
5. Zhou, S., Yang, Z., Liu, J. & Ran, M. TIPE-2 ameliorates inflammatory bowel disease in mice via inhibiting STAT3 and NF-kB activation. *Immunol. Lett.* **255**, 32–39 (2023).
6. Zhao, C., Xiao, C., Feng, S. & Bai, J. Artemisitene alters LPS-induced oxidative stress, inflammation and ferroptosis in liver through Nrf2/HO-1 and NF-kB pathway. *Front. Pharmacol.* **14**, 1177542 (2023).
7. Rajendran, P. et al. Nimbolide: promising agent for prevention and treatment of chronic diseases (recent update). *Food Nutr. Res.* **68**, 10–29219 (2024).
8. Li, J. et al. Discovery of anti-inflammatory natural flavonoids: Diverse scaffolds and promising leads for drug discovery. *Eur. J. Med. Chem.* **260**, 115791 (2023).
9. Xue, J. C. et al. The role and mechanism of flavonoid herbal natural products in ulcerative colitis. *Biomed. Pharmacother.* **158**, 114086 (2023).
10. Mabry TJ, Markham KR, Thomas MB, Mabry TJ, Markham KR, Thomas MB. The ultraviolet spectra of flavones and flavonols. In: The Systematic Identification of Flavonoids. Springer, Berlin. https://doi.org/10.1007/978-3-642-88458-0_5
11. Mabry, T., Markham, K. R. & Thomas, M. B. *The Systematic Identification of Flavonoids* (Springer Science & Business Media, Cham, 2012).
12. Lin, L. J., Huang, X. B. & Lv, Z. C. Isolation and identification of flavonoids components from *Pteris vittata* L.. *Springerplus* **5**, 1–3 (2016).
13. Reddy, M. V., Reddy, M. K., Gunasekar, D., Caux, C. & Bodo, B. A flavanone and a dihydrodibenzoxepin from Bauhinia variegata. *Phytochemistry* **64**, 879–882 (2003).
14. Papa, A. et al. Gut dysbiosis-related thrombosis in inflammatory bowel disease: Potential disease mechanisms and emerging therapeutic strategies. *Thromb. Res.* **232**, 77–88 (2023).
15. Lam, I. H., Chan, C. I., Han, M., Li, L. & Yu, H. H. ACSL4 mediates inflammatory bowel disease and contributes to LPS-induced intestinal epithelial cell dysfunction by activating ferroptosis and inflammation. *Open Med.* **19**, 20240993 (2024).
16. Qu, Y. et al. Kaempferol alleviates murine experimental colitis by restoring gut microbiota and inhibiting the LPS-TLR4-NF-κB axis. *Front. Immunol.* **12**, 679897 (2021).
17. Saxena, S. & Chakraborty, D. Antioxidant activity and GC-MS analysis of *Bauhinia variegata* L. (Fabaceae). *Res. J. Pharm. Technol.* **17**, 208–212 (2024).
18. Bhargav, M. D. Isolation and characterization of major phytochemical constituents from *Bauhinia variegata* leaf extract. *J. Pharmac. Res.* **18**(4), 2 (2019).
19. Zhang, Q.-W., Lin, L.-G. & Ye, W.-C. Techniques for extraction and isolation of natural products: A comprehensive review. *Chinese Medicine* **13**, 20 (2018).
20. Chen, X. et al. Dimethyl sulfoxide inhibits bile acid synthesis in healthy mice but does not protect mice from bile-acid-induced liver damage. *Biology.* **12**(8), 1105 (2023).
21. Li, X. et al. Oligosaccharides isolated from *Rehmannia glutinosa* protect LPS-induced intestinal inflammation and barrier injury in mice. *Front. Nutr.* **23**(10), 1139006 (2023).
22. Bhardwaj, M., Sali, V. K., Mani, S. & Vasanthi, H. R. Neophytadiene from *Turbinaria ornata* suppresses LPS-induced inflammatory response in RAW 264.7 macrophages and Sprague Dawley rats. *Inflammation* **43**(3), 937–950 (2020).
23. Velisetty VP, Subhashini PK, Reddy YB, Prapanna V. Evaluation of Carrageenan Induced Anti-Inflammatory & Anti Pyretic Activity of Various Extracts of Bauhina Variegata Linn in Rats.
24. Saha S, Subrahmanyam EV. Evaluation of immunomodulatory effect of aqueous extract of *Bauhinia variegata* L. leaves. Indian J. Pharmac. Edu. Res. 2023; 57.
25. Rajendran, P. Unveiling the power of flavonoids: A dynamic exploration of their impact on cancer through matrix metalloproteinases regulation. *Biomedicine* **14**, 12 (2024).
26. Shen, N. et al. Plant flavonoids: Classification, distribution, biosynthesis, and antioxidant activity. *Food Chem.* **383**, 132531 (2022).
27. Vissenaekens, H. et al. Flavonoids and cellular stress: A complex interplay affecting human health. *Crit. Rev. Food Sci. Nutr.* **62**, 8535–8566 (2022).
28. Chen, Y. et al. Dietary proanthocyanidins on gastrointestinal health and the interactions with gut microbiota. *Crit. Rev. Food Sci. Nutr.* **63**, 6285–6308 (2023).
29. Oteiza, P. I., Fraga, C. G., Mills, D. A. & Taft, D. H. Flavonoids and the gastrointestinal tract: Local and systemic effects. *Mol. Aspects Med.* **61**, 41–49 (2018).
30. Liu, Y. H., Li, X. Y., Chen, C. Y., Zhang, H. M. & Kang, J. X. Omega-3 fatty acid intervention suppresses lipopolysaccharide-induced inflammation and weight loss in mice. *Mar. Drugs* **13**, 1026–1036 (2015).
31. Yoo, D. K. & Lee, S. H. Effect of lipopolysaccharide (LPS) exposure on the reproductive organs of immature female rats. *Dev. Reprod.* **20**, 113 (2016).
32. Straub, R. H., Cutolo, M., Buttgereit, F. & Pongratz, G. Energy regulation and neuroendocrine–immune control in chronic inflammatory diseases. *J. Intern. Med.* **267**, 543–560 (2010).
33. Kamboh, A. A., Hang, S. Q., Khan, M. A. & Zhu, W. Y. In vivo immunomodulatory effects of plant flavonoids in lipopolysaccharide-challenged broilers. *Animal* **10**, 1619–1625 (2016).
34. Yuan, L. et al. Effects of natural flavonoid isoorientin on growth performance and gut microbiota of mice. *J. Agric. Food Chem.* **66**, 9777–9784 (2018).
35. Yue, C., Ma, B., Zhao, Y., Li, Q. & Li, J. Lipopolysaccharide-induced bacterial translocation is intestine site-specific and associates with intestinal mucosal inflammation. *Inflammation* **35**, 1880–1888 (2012).
36. Ghosh, S. S., Wang, J., Yannie, P. J. & Ghosh, S. Intestinal barrier dysfunction, LPS translocation, and disease development. *J. Endocrine Soc.* **4**, 039 (2020).
37. Pinho-Ribeiro, F. A. et al. The citrus flavonone naringenin reduces lipopolysaccharide-induced inflammatory pain and leukocyte recruitment by inhibiting NF-κB activation. *J. Nutr. Biochem.* **33**, 8–14 (2016).
38. Chagas, M. D. et al. Flavonols and flavones as potential anti-inflammatory, antioxidant, and antibacterial compounds. *Oxidative Med. Cell. Longevity.* **2022**(1), 9966750 (2022).
39. Kłósek, M. et al. In vitro anti-inflammatory activity of methyl derivatives of flavanone. *Molecules* **28**, 7837 (2023).
40. Chen, C. et al. Dietary citrus flavonoids improved growth performance and intestinal microbiota of weaned piglets via immune function mediated by TLR2/NF-κB signaling pathway. *J. Agric. Food Chem.* **72**, 16761–16776 (2024).
41. Luo, D. et al. Naringin mitigates LPS-induced intestinal barrier injury in mice. *Food Funct.* **14**, 1617–1626 (2023).
42. Noworyta-Sokołowska, K., Górska, A. & Gołembiowska, K. LPS-induced oxidative stress and inflammatory reaction in the rat striatum. *Pharmacol. Rep.* **65**, 863–869 (2013).
43. Wei, L., Li, Y., Chang, Q., Guo, G. & Lan, R. Effects of chitosan oligosaccharides on intestinal oxidative stress and inflammation response in heat stressed rats. *Exp. Anim.* **70**, 45–53 (2021).

44. Liu, W. Y., Liou, S. S., Hong, T. Y. & Liu, I. M. Protective effects of hesperidin (*citrus flavonone*) on high glucose induced oxidative stress and apoptosis in a cellular model for diabetic retinopathy. *Nutrients* **9**, 1312 (2017).
45. Zaidun, N. H., Thent, Z. C. & Abd, L. A. Combating oxidative stress disorders with citrus flavonoid: Naringenin. *Life Sci.* **208**, 111–122 (2018).
46. Park, S. H., Pradeep, K. & Ko, K. C. Protective effect of hesperidin against γ-radiation induced oxidative stress in Sprague–Dawley rats. *Pharm. Biol.* **47**, 940–947 (2009).
47. Liu, Y. et al. TMF Attenuates cognitive impairment and neuroinflammation by inhibiting the MAPK/NF-κB pathway in Alzheimer's disease: A multi-omics analysis. *Mar. Drugs* **23**, 74 (2025).

Author contributions
PR conceived the project. PR, BR, and RS designed the study. PR, BR, LKG, FAA, GMB, AMMI and MNN performed the experiments, analyzed the data and edited the manuscript. PR wrote the first draft of the manuscript. RS revised and edited the final draft.

Institutional review board statement
The in vivo animal experiments were approved and licensed by the Research Ethics Committee, Deanship of Scientific Research at King Faisal University (ETHICS2464).

Funding
The authors extend their appreciation to the Deanship of Scientific Research, Vice Presidency for Graduate Studies and Scientific Research, King Faisal University, Saudi Arabia, for funding this research work (project number KFU253887).

Competing interests
The authors declare no competing interests.

Additional information
Supplementary Information The online version contains supplementary material available at https://doi.org/10.1038/s41598-025-26900-6.

Correspondence and requests for materials should be addressed to P.R. or R.S.

Reprints and permissions information is available at www.nature.com/reprints.

Publisher's note Springer Nature remains neutral with regard to jurisdictional claims in published maps and institutional affiliations.

Open Access This article is licensed under a Creative Commons Attribution-NonCommercial-NoDerivatives 4.0 International License, which permits any non-commercial use, sharing, distribution and reproduction in any medium or format, as long as you give appropriate credit to the original author(s) and the source, provide a link to the Creative Commons licence, and indicate if you modified the licensed material. You do not have permission under this licence to share adapted material derived from this article or parts of it. The images or other third party material in this article are included in the article's Creative Commons licence, unless indicated otherwise in a credit line to the material. If material is not included in the article's Creative Commons licence and your intended use is not permitted by statutory regulation or exceeds the permitted use, you will need to obtain permission directly from the copyright holder. To view a copy of this licence, visit http://creativecommons.org/licenses/by-nc-nd/4.0/.

© The Author(s) 2025